

# The effect of nonuniform beam filling on the quality of radar polarimetric data

Alexander Ryzhkov

University of Oklahoma / National Severe Storms Laboratory, Norman (USA)

## 1 Introduction

One of the reasons for gradual degradation of the quality of radar polarimetric information with range is progressive beam broadening and stronger impact of nonuniform beam filling (NBF).

Nonuniform beam filling may also cause significant perturbations of the radial profile of differential phase  $\Phi_{DP}$  (Ryzhkov and Zrnicek 1998; Gosset 2004). Such perturbations of  $\Phi_{DP}$  result in spurious values of its radial derivative, specific differential phase  $K_{DP}$ , and strong biases in the  $K_{DP}$ -based estimates of rain rate. These adverse effects are commonly manifested as the appearance of negative  $K_{DP}$  in the regions of strongly nonuniform precipitation and become more pronounced as the physical size of the radar resolution volume increases at longer distances.

The magnitude of the cross-correlation coefficient  $\rho_{hv}$  is closely related to the distribution of differential phase within the radar resolution volume. Large cross-beam gradients of  $\Phi_{DP}$  may cause noticeable decrease of  $\rho_{hv}$  which is, in its turn, accompanied by higher statistical errors in the measurements of all polarimetric variables.

In this paper, the effects of beam broadening on polarimetric measurements are quantified using a simple model of nonuniform beam filling. It is assumed that the antenna patterns at the two orthogonal polarizations are perfectly matched and the biases of the measured  $Z_{DR}$ ,  $\Phi_{DP}$ , and  $\rho_{hv}$  are solely due to linear cross-beam gradients of different radar variables.

## 2 Theoretical analysis

In the case of weather scatterers, the voltage vectors of the transmitted ( $\mathbf{V}^t$ ) and received ( $\mathbf{V}$ ) waves are related as

$$\begin{pmatrix} V_h \\ V_v \end{pmatrix} = C_1 \begin{pmatrix} T_{hh} & 0 \\ 0 & T_{vv} \end{pmatrix} \begin{pmatrix} S_{hh} & S_{hv} \\ S_{hv} & S_{vv} \end{pmatrix} \begin{pmatrix} T_{hh} & 0 \\ 0 & T_{vv} \end{pmatrix} \begin{pmatrix} V_h^t \\ V_v^t \end{pmatrix}, \quad (1)$$

where matrix elements  $S_{hh}$ ,  $S_{vv}$ , and  $S_{hv}$  represent backscattering coefficients of hydrometeors in the radar resolution volume and  $T_{hh}$  and  $T_{vv}$  describe phase shifts and attenuations for H and V waves along propagation path

$$T_{hh,vv} = \exp(-j\Phi_{h,v} - \Gamma_{h,v}) \quad , \quad (2)$$

where  $\Phi_{h,v}$  is phase shift and  $\Gamma_{h,v}$  is attenuation. Differential phase  $\Phi_{DP}$  is defined as

$$\Phi_{DP} = 2(\Phi_h - \Phi_v) \quad . \quad (3)$$

The coefficient  $C_1$  is a constant depending on radar parameters and range from the scatterers. If both H and V waves are transmitted simultaneously (i.e.  $\mathbf{V}^t = (V_h^t, V_v^t)$ ) and the cross-coupling terms proportional to  $S_{hv}$  are neglected (which is reasonable assumption for rain and aggregated snow (Doviak et al. 2000)), then

$$V_h = C_1 T_{hh}^2 S_{hh} V^t \quad \text{and} \quad V_v = C_1 T_{vv}^2 S_{vv} V^t \quad . \quad (4)$$

Using (4), we introduce effective radar reflectivity factors  $Z_{h,v}^{(e)}$  at orthogonal polarizations as

$$Z_{h,v}^{(e)} = C_2 \overline{|V_{h,v}|^2} = Z_{h,v} e^{-4\Gamma_{h,v}} \quad , \quad (5)$$

effective differential reflectivity

$$Z_{dr}^{(e)} = \frac{Z_h^{(e)}}{Z_v^{(e)}} = Z_{dr} e^{-4(\Gamma_h - \Gamma_v)} \quad , \quad (6)$$

Correspondence to: Alexander Ryzhkov

[Alexander.Ryzhkov@noaa.gov](mailto:Alexander.Ryzhkov@noaa.gov)

and the covariance

$$R_{hv} = C_2 \overline{V_h^* V_v} = Z_{hv} e^{j\Phi_{DP}'} , \quad (7)$$

where

$$Z_{hv} = (Z_h Z_v)^{1/2} |\rho_{hv}| e^{-2(\Gamma_h + \Gamma_v)} , \quad (8)$$

$$\Phi_{DP}' = \Phi_{DP} + \arg(\rho_{hv}) . \quad (9)$$

In (5) – (9), intrinsic values of radar reflectivities  $Z_{h,v}$ , differential reflectivity  $Z_{dr}$ , and cross-correlation coefficient  $\rho_{hv}$  are defined from the second moments of the scattering matrix  $\mathbf{S}$ :

$$\begin{aligned} Z_h &= C' \langle |S_{hh}|^2 \rangle, \quad Z_v = C' \langle |S_{vv}|^2 \rangle, \\ Z_{dr} &= \frac{\langle |S_{hh}|^2 \rangle}{\langle |S_{vv}|^2 \rangle}, \quad \rho_{hv} = \frac{\langle S_{hh}^* S_{vv} \rangle}{\langle |S_{hh}|^2 \rangle^{1/2} \langle |S_{vv}|^2 \rangle^{1/2}} \end{aligned} \quad (10)$$

Overbars in Eq (5) and (7) mean expected values, brackets in (10) stand for ensemble averaging. The factors  $C_2$  and  $C'$  are constants.

The radar measured reflectivities  $Z_{h,v}^{(m)}$  and the covariance  $R_{hv}^{(m)}$  are weighted by the radar antenna pattern  $I(\mathbf{r}, \mathbf{r}_0)$  as follows:

$$Z_{h,v}^{(m)}(\mathbf{r}_0) = \int Z_{h,v}^{(e)}(\mathbf{r}) I(\mathbf{r}, \mathbf{r}_0) d\mathbf{r} \quad (11)$$

$$R_{hv}^{(m)}(\mathbf{r}_0) = \int R_{hv}(\mathbf{r}) I(\mathbf{r}, \mathbf{r}_0) d\mathbf{r} \quad (12)$$

In (11) and (12), it is assumed that antenna patterns are identical at the two orthogonal polarizations. The measured differential phase  $\Phi_{DP}^{(m)}$  and cross-correlation coefficient  $\rho_{hv}^{(m)}$  are

$$\Phi_{DP}^{(m)} = \arg(R_{hv}^{(m)}) \quad \rho_{hv}^{(m)} = \frac{R_{hv}^{(m)}}{(Z_h^{(m)} Z_v^{(m)})^{1/2}} . \quad (13)$$

The values of  $\Phi_{DP}^{(m)}$  and  $\rho_{hv}^{(m)}$  depend on the distributions of  $Z_{h,v}^{(e)}$  and  $R_{hv}$  within the radar resolution volume and on the shape of antenna pattern. In this study, we assume that a two-way antenna power pattern is axisymmetric and Gaussian (Doviak and Zrníc 1993):

$$I(\theta, \varphi) = \frac{1}{2\pi\sigma^2} \exp\left(-\frac{\theta^2 + \varphi^2}{2\sigma^2}\right), \quad (14)$$

where  $\theta$  and  $\varphi$  are elevation and azimuth and  $\sigma = \Omega/4(\ln 2)^{1/2}$  ( $\Omega$  is a one-way 3 dB antenna pattern width).

Next we assume that reflectivity factors  $Z_{h,v}^{(e)}$  and  $Z_{hv}$  expressed in logarithmic scale vary linearly in both cross-beam directions,  $\theta$  and  $\varphi$ :

$$10 \log(Z_{h,v}^{(e)}(\theta, \varphi)) = Z_{H,V}^{(e)}(0,0) + \frac{dZ_{H,V}^{(e)}}{d\theta} \theta + \frac{dZ_{H,V}^{(e)}}{d\varphi} \varphi \quad (15)$$

$$10 \log(Z_{hv}(\theta, \varphi)) = Z_{HV}(0,0) + \frac{dZ_{HV}}{d\theta} \theta + \frac{dZ_{HV}}{d\varphi} \varphi \quad (16)$$

Similar assumption is made for differential phase  $\Phi_{DP}'$ :

$$\Phi_{DP}'(\theta, \varphi) = \Phi_{DP}'(0,0) + \frac{d\Phi_{DP}'}{d\theta} \theta + \frac{d\Phi_{DP}'}{d\varphi} \varphi . \quad (17)$$

Integrating (11) and (12), one can obtain the following approximate formulas for the biases of  $Z_{DR}$ ,  $\Phi_{DP}$ , and  $\rho_{hv}$ :

$$\Delta Z_{DR} = 0.02 \Omega^2 \left( \frac{dZ_H^{(e)}}{d\theta} \frac{dZ_{DR}^{(e)}}{d\theta} + \frac{dZ_H^{(e)}}{d\varphi} \frac{dZ_{DR}^{(e)}}{d\varphi} \right) \quad (18)$$

$$\Delta \Phi_{DP} = 0.02 \Omega^2 \left( \frac{d\Phi_{DP}'}{d\theta} \frac{dZ_{HV}^{(e)}}{d\theta} + \frac{d\Phi_{DP}'}{d\varphi} \frac{dZ_{HV}^{(e)}}{d\varphi} \right) \quad (19)$$

$$\frac{|\rho_{hv}^{(m)}|}{|\rho_{hv}|} = \exp \left\{ -1.37 \cdot 10^{-5} \Omega^2 \left[ \left( \frac{d\Phi_{DP}'}{d\theta} \right)^2 + \left( \frac{d\Phi_{DP}'}{d\varphi} \right)^2 \right] \right\} \quad (20)$$

In Eqs. (18) – (20),  $\Phi_{DP}'$ ,  $\Delta \Phi_{DP}$ ,  $\Omega$ ,  $\theta$ , and  $\varphi$  are expressed in degrees, whereas  $Z_H$ ,  $Z_{HV}$ ,  $\Delta Z_{DR}$ , and  $Z_{DR}$  are in dB.

### 3 Nonuniform beam filling effects in the case of mesoscale convective system

The gradients of  $Z_H$ ,  $Z_{HV}$ ,  $Z_{DR}$ , and  $\Phi_{DP}$  in Eqs. (18) – (20) can be approximately estimated from real data by comparing the corresponding variables at adjacent radials. We perform such estimation in the case of a mesoscale convective system that was observed with the polarimetric prototype of the S-band WSR-88D radar (KOUN hereafter) in central Oklahoma on June 2, 2004. The analysis was conducted using the data from two lowest PPIs at elevations  $0.44^\circ$  and  $1.45^\circ$ . Horizontal gradients were computed from the data collected at the lowest elevation, whereas vertical gradients were estimated using the data at both elevations.

Composite plot of  $Z_H$ ,  $Z_{DR}$ ,  $\Phi_{DP}$ , and  $1-\rho_{hv}$  at elevation  $0.44^\circ$  exhibits strong squall line followed by stratiform trailing precipitation on 2231 UTC (Fig. 1). Differential reflectivity in the squall line decreases with distance from the radar as the dominant scatterers in the radar resolution volume change from raindrops to graupel. Differential phase grows only modestly in the convective part of the storm because the squall line is viewed at an angle by the radar. The only suspicious signature is a noticeable drop in the cross-correlation coefficient at  $X > 100$  km and  $Y < -100$  km.

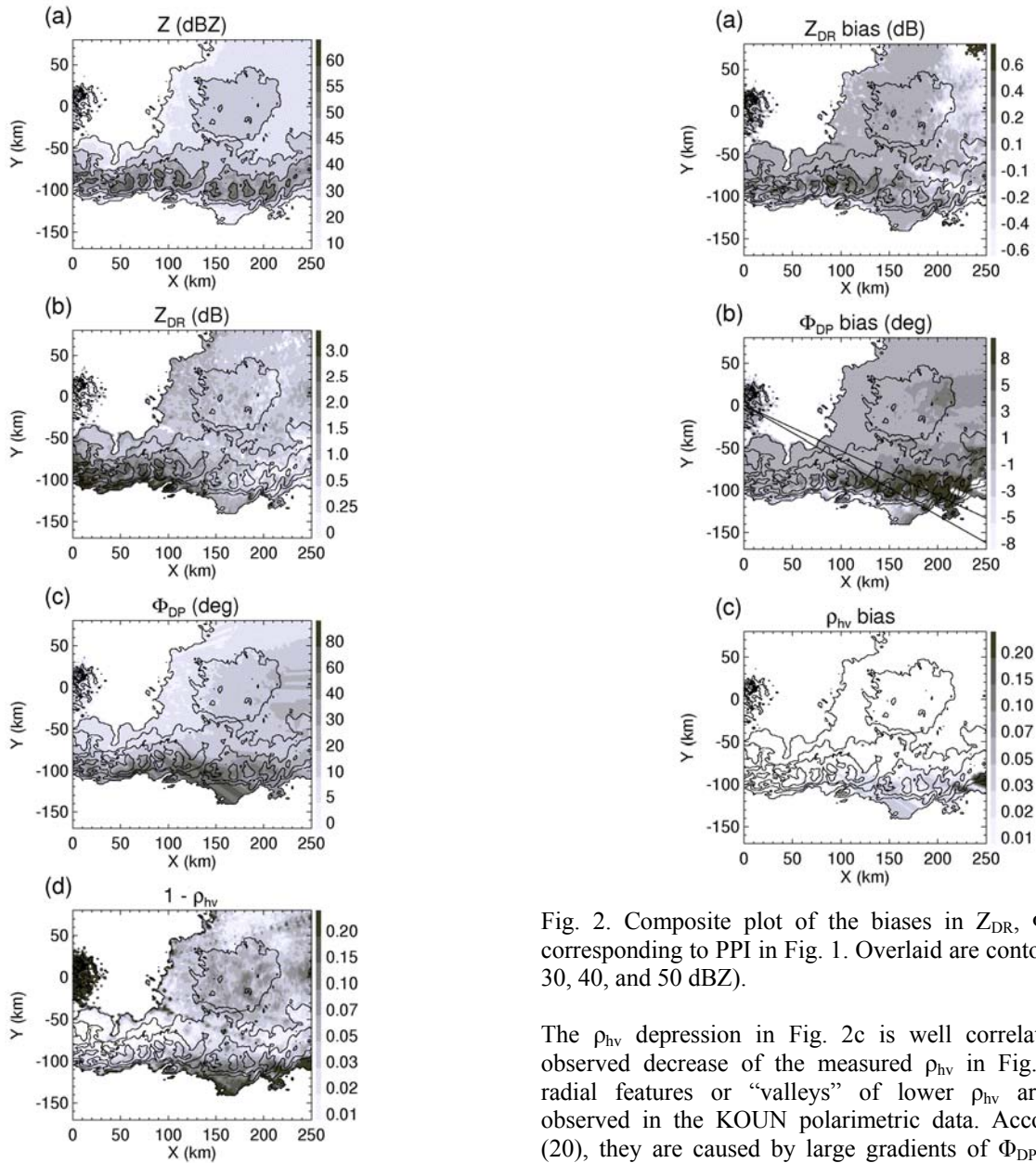


Fig. 1. Composite plot of  $Z$ ,  $Z_{DR}$ ,  $\Phi_{DP}$ , and  $1 - \rho_{hv}$  measured by the KOUN WSR-88D radar on 06/02/2004 at 2231 UTC. Elevation is  $0.44^\circ$ . Overlaid are contours of  $Z$  (10, 30, 40, and 50 dBZ).

The fields of the biases of  $Z_{DR}$ ,  $\Phi_{DP}$ , and  $\rho_{hv}$  computed from the estimated gradients of  $Z$ ,  $Z_{DR}$ , and  $\Phi_{DP}$  using Eqs (18) – (20) reveal quite serious errors in the estimates of polarimetric variables (Fig. 2). The NBF-related bias in  $Z_{DR}$  exceeds several tenths of dB in some parts of the storm as Fig. 2a shows. Biases of  $\Phi_{DP}$  of both signs with magnitudes larger than  $10^\circ$  are also common.

Fig. 2. Composite plot of the biases in  $Z_{DR}$ ,  $\Phi_{DP}$ , and  $\rho_{hv}$  corresponding to PPI in Fig. 1. Overlaid are contours of  $Z$  (10, 30, 40, and 50 dBZ).

The  $\rho_{hv}$  depression in Fig. 2c is well correlated with the observed decrease of the measured  $\rho_{hv}$  in Fig. 1d. Similar radial features or “valleys” of lower  $\rho_{hv}$  are frequently observed in the KOUN polarimetric data. According to Eq (20), they are caused by large gradients of  $\Phi_{DP}$  that usually monotonically increase with range.

The biases or perturbations of  $\Phi_{DP}$  are determined by both the gradients of differential phase and reflectivity factor. As a result,  $\Delta\Phi_{DP}$  exhibits more complex and nonmonotonic behavior along the radial than the  $\rho_{hv}$  bias. The perturbations of the  $\Phi_{DP}$  radial profiles are generally in good agreement with their estimates from the gradients in accordance with Eq. (19). Such an agreement is well illustrated in Fig. 3 where measured range dependencies of  $\Phi_{DP}$  (thin curves) are compared with radial profiles of  $\Delta\Phi_{DP}$  calculated from Eq (19) (thick curves) for six successive azimuths belonging to the sector indicated in Fig. 2b.

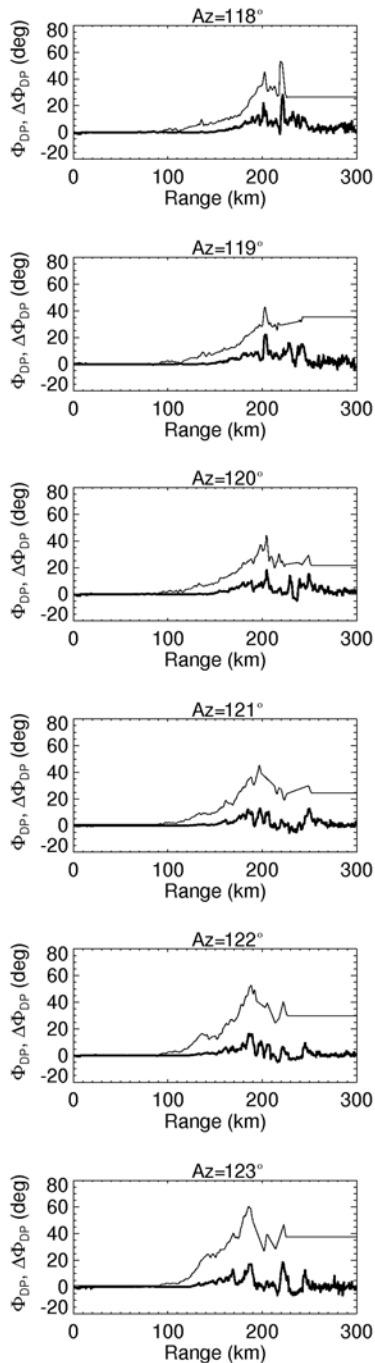


Fig. 3. Radial profiles of  $\Phi_{DP}$  (thin curves) and its bias ( $\Delta\Phi_{DP}$ , thick curves) caused by nonuniform beam filling at six adjacent azimuths within the sector shown in Fig. 2b.

Despite many simplified assumptions made in evaluation of  $\Delta\Phi_{DP}$ , correlation between the  $\Phi_{DP}$  and  $\Delta\Phi_{DP}$  profiles is surprisingly high. Most pronounced excursions of the  $\Phi_{DP}$  curves, such as spikes and depressions are well reproduced in the modeled  $\Delta\Phi_{DP}$ . Thus, they are primarily attributed to

nonuniform beam filling rather than pure statistical errors in  $\Phi_{DP}$  estimation or to the contribution from backscatter differential phase.

#### 4 Discussion and summary

The biases of  $\Phi_{DP}$  and  $\rho_{hv}$  are wavelength-dependent because differential phase and its gradients are inversely proportional to the radar wavelength  $\lambda$ . The impact on  $\Delta\Phi_{DP}$  is proportional to  $\lambda^{-1}$ , whereas the  $\rho_{hv}$  bias is approximately proportional to  $\lambda^{-2}$ . Enhanced attenuation and differential attenuation at shorter wavelengths may either increase or decrease the gradients of  $Z$  and  $Z_{DR}$ . In some situations, these changes in the  $Z$  and  $Z_{DR}$  gradients may offset the increase in the gradient of  $\Phi_{DP}$  and its greater impact on the NBF-related biases in  $\Phi_{DP}$  and  $\rho_{hv}$ . However, cursory analysis of the C-band and X-band simulated and observed polarimetric data reveals stronger nonuniform beam filling effects compared to S band (Ryzhkov and Zrnice 2005).

The magnitudes of  $\Delta Z_{DR}$ ,  $\Delta\Phi_{DP}$ , and  $\Delta\rho_{hv}$  depend on the square of antenna beamwidth. Such a strong dependence may preclude the use of wide-beam antennas for polarimetric measurements.

We emphasize that formulas (18) – (20) can not be used for correction of  $Z_{DR}$ ,  $\Phi_{DP}$ , and  $\rho_{hv}$  because the bias estimates are very approximate due to many simplifying assumptions made in derivation of these equations. Instead, we recommend using  $\Delta Z_{DR}$ ,  $\Delta\Phi_{DP}$ , and  $\Delta\rho_{hv}$  as *quality indexes* for the corresponding radar variables. Such an approach is used in the algorithms for hydrometeor classification and rainfall estimation developed at NSSL for operational utilization with the polarimetric prototype of the WSR-88D radar.

#### References

- Doviak, R.J., and D.S. Zrnice, 1993: *Doppler Radar and Weather Observations*. 2d ed. Academic Press, 562 pp.
- Doviak, R.J., V. Bringi, A.V. Ryzhkov, A. Zahrai, D.S. Zrnice, 2000: Considerations for polarimetric upgrades to operational WSR-88D radars. *J. Atmos. Oceanic Technol.*, **17**, 257 - 278.
- Gosset, M., 2004: Effect of nonuniform beam filling on the propagation of radar signals at X-band frequencies. Pt II. Examination of differential phase shift. *J. Atmos. Oceanic Technol.*, **21**, 358 – 367.
- Ryzhkov, A., and D. Zrnice, 1998: Beamwidth effects on the differential phase measurements of rain. *J. Atmos. Oceanic Technol.*, **15**, 624 – 634.
- Ryzhkov, A.V., and D.S. Zrnice, 2005: Radar polarimetry at S, C, and X bands. Comparative analysis and operational implications. Preprints, *32<sup>nd</sup> Conference on Radar Meteorology*, Albuquerque, NM, Amer. Meteor. Soc., CD-ROM, 9R.3.